Physics Letters B 749 (2015) 50–56

Contents lists available at ScienceDirect

Physics Letters B

www.elsevier.com/locate/physletb

Final analysis of KEDR data on J/ψ and $\psi(2S)$ masses

V.V. Anashin [a], V.M. Aulchenko [a,b], E.M. Baldin [a,b], A.K. Barladyan [a], A.Yu. Barnyakov [a,b], M.Yu. Barnyakov [a,b], S.E. Baru [a,b], I.Yu. Basok [a], A.M. Batrakov [a], A.E. Blinov [a,b], V.E. Blinov [a,b,c], A.V. Bobrov [a,b], V.S. Bobrovnikov [a,b], A.V. Bogomyagkov [a,b], A.E. Bondar [a,b], A.A. Borodenko [a], A.R. Buzykaev [a,b], S.I. Eidelman [a,b], D.N. Grigoriev [a,b,c], Yu.M. Glukhovchenko [a], S.E. Karnaev [a], G.V. Karpov [a], S.V. Karpov [a], T.A. Kharlamova [a], V.A. Kiselev [a], V.V. Kolmogorov [a], S.A. Kononov [a,b], K.Yu. Kotov [a], E.A. Kravchenko [a,b], V.N. Kudryavtsev [a,b], V.F. Kulikov [a,b], G.Ya. Kurkin [a,c], I.A. Kuyanov [a], E.A. Kuper [a,b], E.B. Levichev [a,c], D.A. Maksimov [a,b], V.M. Malyshev [a], A.L. Maslennikov [a,b], O.I. Meshkov [a,b], S.I. Mishnev [a], I.I. Morozov [a,b], N.Yu. Muchnoi [a,b], V.V. Neufeld [a], S.A. Nikitin [a], I.B. Nikolaev [a,b], I.N. Okunev [a], A.P. Onuchin [a,b,c], S.B. Oreshkin [a], A.A. Osipov [a,b], I.V. Ovtin [a,c], S.V. Peleganchuk [a,b], S.G. Pivovarov [a,c], P.A. Piminov [a], V.V. Petrov [a], V.G. Prisekin [a,b], O.L. Rezanova [a,b], A.A. Ruban [a,b], V.K. Sandyrev [a], G.A. Savinov [a], A.G. Shamov [a,b,*], D.N. Shatilov [a], B.A. Shwartz [a,b], E.A. Simonov [a], S.V. Sinyatkin [a], A.N. Skrinsky [a], A.V. Sokolov [a,b], A.M. Sukharev [a,b], E.V. Starostina [a,b], A.A. Talyshev [a,b], V.A. Tayursky [a,b], V.I. Telnov [a,b], Yu.A. Tikhonov [a,b], K.Yu. Todyshev [a,b], G.M. Tumaikin [a], Yu.V. Usov [a], A.I. Vorobiov [a], V.N. Zhilich [a,b], V.V. Zhulanov [a,b], A.N. Zhuravlev [a,b]

[a] *Budker Institute of Nuclear Physics, 11, akademika Lavrentieva prospect, Novosibirsk, 630090, Russia*
[b] *Novosibirsk State University, 2, Pirogova street, Novosibirsk, 630090, Russia*
[c] *Novosibirsk State Technical University, 20, Karl Marx prospect, Novosibirsk, 630092, Russia*

ARTICLE INFO

Article history:
Received 6 May 2015
Received in revised form 11 July 2015
Accepted 22 July 2015
Available online 28 July 2015
Editor: M. Doser

ABSTRACT

We present the analysis of all KEDR data on the determination of J/ψ and $\psi(2S)$ masses. The data comprise six scans of J/ψ and seven scans of $\psi(2S)$ which were performed at the VEPP-4M e^+e^- collider in 2002–2008. The beam energy was determined using the resonance depolarization method. The detector and accelerator conditions during scans were very different that increases the reliability of the averaged results. The analysis accounts for partial correlations of systematic uncertainties on the masses. The following mass values were obtained:

$$M_{J/\psi} = 3096.900 \pm 0.002 \pm 0.006 \text{ MeV}, \qquad M_{\psi(2S)} = 3686.099 \pm 0.004 \pm 0.009 \text{ MeV}.$$

These results supersede our previous measurements published in 2003 and 2012.

1. Introduction

The mass of a particle is its most fundamental characteristic which should be known with the best possible accuracy. The masses of the very narrow J/ψ and $\psi(2S)$ mesons are applied to the calibration of energy scales of accelerators and detectors operating in the charmonium region, thus their precision is among the factors determining the accuracy of results on masses of the other charmonium states and of the τ-lepton. Some recent examples of such applications are the precision measurement of the τ-lepton mass at BEPC-II [1], the high precision measurement of the masses of the D^0 and K_S mesons [2] and the determination of the binding energy of $X(3872)$ [3] using the data collected by CLEO-c.

* Corresponding author at: Budker Institute of Nuclear Physics, 11, akademika Lavrentieva prospect, Novosibirsk, 630090, Russia.
E-mail address: a.g.shamov@inp.nsk.su (A.G. Shamov).

http://dx.doi.org/10.1016/j.physletb.2015.07.057

The first precision measurement of J/ψ and $\psi(2S)$ masses was performed with the OLYA detector at the VEPP-4 e^+e^- collider in 1980 [4] employing the resonance depolarization method [5, 6] invented five years earlier. The accuracy of about 100 keV was achieved. Using the $\psi(2S)$ mass value obtained by OLYA for the calibration of the Fermilab Antiproton Accumulator ring's orbit length, the E760 experiment has reached the accuracy of about 40 keV on the J/ψ mass [7]. It was possible because of a non-linear relation between the orbit length and the invariant mass of the antiproton of the beam and the proton of the internal gas jet target.

The improvement of the energy measurement technique at the upgraded VEPP-4M e^+e^- collider and thorough analysis of systematic uncertainties allowed for the further increase of the accuracy on masses of the narrow ψ states. The accuracy achieved in the KEDR experiment [8] was about 12 and 27 keV for J/ψ and $\psi(2S)$, respectively. Later, when the liquid krypton calorimeter was installed in the KEDR detector and three additional scans of the $\psi(2S)$ region were performed, the $\psi(2S)$ mass accuracy was improved to 17 keV [9].

Besides the J/ψ and $\psi(2S)$ measurements mentioned above, the current Review of Particle Physics [10] contains the recent result of the LHCb Collaboration on $\psi(2S)$ mass which has the accuracy of about 110 keV [11]. The current world average values $M_{J/\psi} = 3096.916 \pm 0.011$ and $M_{\psi(2S)} = 3686.108^{+0.011}_{-0.014}$ MeV are dominated by results of Refs. [8] and [9].

In this paper we present the analysis of six scans of J/ψ and seven scans of $\psi(2S)$ performed at the VEPP-4M collider under different detector and accelerator conditions. In all scans the beam energy was determined using the resonance depolarization method.

The resonance masses were determined by fitting the inclusive hadronic cross sections as a function of the e^+e^- center-of-mass (c.m.) energy.

2. VEPP-4M collider and KEDR detector

The VEPP-4M e^+e^- collider [12] consists of the booster ring VEPP-3 with energy up to 2000 MeV and the main ring operating in the beam energy range from 1 GeV to 5.5 GeV. The peak luminosity in the 2×2 bunches operation mode is about 2×10^{30} cm^{-2} s^{-1} in the ψ region. The electron and positron beams rotate in VEPP-4M in the same ring which facilitates high precision determination of collision energy as discussed below in Section 6.

The KEDR detector [13] (Fig. 1) comprises the vertex detector (VD), drift chamber (DC), time-of-flight (TOF) system of scintillation counters, particle identification system based on the aerogel Cherenkov counters, EM calorimeter (liquid krypton in the barrel part and CsI crystals in the endcaps), superconducting magnet system and muon system inside the magnet yoke. The superconducting solenoid provides a longitudinal magnetic field of up to 0.7 T. The detector is equipped with a scattered electron tagging system for two-photon studies. The on-line luminosity measurement is provided by two independent single bremsstrahlung monitors.

3. Theoretical e^+e^- cross section in vicinity of a narrow resonance

According to Ref. [14] the cross section of the single photon annihilation of an e^+e^- pair to a specific state can be written as

$$\sigma(s) = \int dx \, \frac{\sigma_0((1-x)s)}{|1-\Pi((1-x)s)|^2} \, \mathcal{F}(s,x), \qquad (1)$$

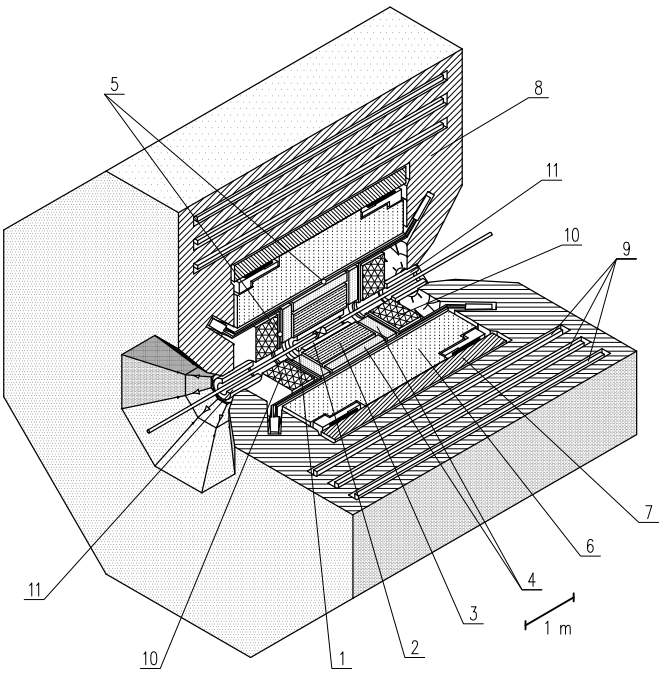

Fig. 1. The KEDR detector. 1 – Vacuum chamber, 2 – Vertex detector, 3 – Drift chamber, 4 – Threshold aerogel counters, 5 – TOF-counters, 6 – Liquid krypton calorimeter, 7 – Superconducting solenoid, 8 – Magnet yoke, 9 – Muon tubes, 10 – CsI calorimeter, 11 – Compensating superconducting coils.

where $s = W^2$ is the square of the c.m. energy of the pair, Π is the full polarization operator which includes the contribution of all 1^{--} resonances and σ_0 is the Born cross section of the process. The radiative correction kernel $\mathcal{F}(s,x)$ describes the probability to lose the fraction x of s by initial state radiation.

The Born cross section and the polarization operator contain the so-called bare resonance parameters. In the soft photon approximation introducing the dressed (physical) resonance parameters M, Γ and Γ_{ee} (the mass, the full width and the electron width) one can obtain the analytical expression for the contribution of a narrow resonance in the inclusive hadronic cross section:

$$\sigma^{\rm hadr}_{\rm n.r.}(W) = \frac{12\pi}{W^2}\,(1+\delta_{\rm sf})\left[\frac{\Gamma_{ee}\tilde{\Gamma}_{\rm h}}{\Gamma M}\,{\rm Im}\, f(W) - \frac{2\alpha\sqrt{R\,\Gamma_{ee}\tilde{\Gamma}_{\rm h}}}{3W}\,\lambda\,{\rm Re}\,\frac{f^*(W)}{1-\Pi_0}\right], \qquad (2)$$

where α is the fine structure constant and R is the ratio $\sigma(e^+e^- \to {\rm hadrons})/\sigma(e^+e^- \to \mu^+\mu^-)$ outside the resonance region. The truncated polarization operator Π_0 does not include a contribution of the resonance itself [15]. The λ parameter characterizes the strength of the interference effect in the inclusive hadronic cross section. Due to the resonance–continuum interference the effective hadronic width $\tilde{\Gamma}_{\rm h}$ can differ from the true hadronic partial width $\Gamma_{\rm h}$.

The correction $\delta_{\rm sf}$ follows from the structure function approach of Ref. [14]:

$$\delta_{\rm sf} = \frac{3}{4}\beta + \frac{\alpha}{\pi}\left(\frac{\pi^2}{3} - \frac{1}{2}\right) + \beta^2\left(\frac{37}{96} - \frac{\pi^2}{12} - \frac{1}{36}\ln\frac{W}{m_e}\right), \qquad (3)$$

$$\beta = \frac{4\alpha}{\pi}\left(\ln\frac{W}{m_e} - \frac{1}{2}\right), \qquad (4)$$

m_e is the electron mass and the function f is defined as

$$f(W) = \frac{\pi\beta}{\sin\pi\beta}\left(\frac{W^2}{M^2 - W^2 - iM\Gamma}\right)^{1-\beta}. \quad (5)$$

The transition from Eq. (1) to Eq. (2), the difference between the bare and dressed resonance parameters and the resonance–continuum interference are considered in Ref. [9]. In particular, the following expression for λ has been obtained:

$$\lambda = \sqrt{\frac{R\mathcal{B}_{ee}}{\mathcal{B}_h}} + \sqrt{\frac{1}{\mathcal{B}_h}}\sum_m \sqrt{b_m \mathcal{B}_m^{(s)}}\,\langle\cos\phi_m\rangle_\Theta\,. \quad (6)$$

The summation is performed over all exclusive hadronic modes. Here $\langle\cos\phi_m\rangle_\Theta$ is the cosine of the relative phase of the strong and electromagnetic amplitudes for the mode m averaged over the phase space of the products, $b_m = R_m/R$ is the branching fraction of the corresponding continuum process, $\mathcal{B}_{ee}$ is the decay probability to an e^+e^- pair, $\mathcal{B}_h$ is the total decay probability to hadrons and $\mathcal{B}_m^{(s)} = \Gamma_m^{(s)}/\Gamma$, where $\Gamma^{(s)}$ is the contribution of the strong interaction to the partial width for the mode m.

In this work we assumed that the relative phases of the strong and electromagnetic amplitudes in different decay modes are not correlated, thus the second term of Eq. (6) can be neglected compared to the first one, which is about 0.39 and 0.13 for J/ψ and $\psi(2S)$, respectively. The experimental verification of this assumption is discussed below in Section 8.

4. Observable e^+e^- cross section

The cross section observed experimentally in the vicinity of a narrow resonance can be parameterized as follows:

$$\sigma_{\text{n.r.}}^{\text{obs}}(W) = \varepsilon\int \sigma_{\text{n.r.}}(W')\,G(W,W')\,dW' + \sigma_{\text{cont}}^{\text{obs}}\cdot(W_{\text{ref}}/W)^2\,. \quad (7)$$

Here ε is the detection efficiency, which can be considered constant and $\sigma_{\text{cont}}^{\text{obs}}$ is the observed continuum cross section in some reference point W_{ref}.

The theoretical cross section $\sigma_{\text{n.r.}}$ is folded with the distribution over the total collision energy which is assumed to be a quasi-Gaussian with an energy spread σ_W:

$$G(W,W') = \frac{g(W-W')}{\sqrt{2\pi}\sigma_W}\exp\left(-\frac{(W-W')^2}{2\sigma_W^2}\right). \quad (8)$$

The preexponential factor is due to accelerator effects, which are discussed in the next section. In the first approximation

$$g(\Delta) = \frac{1 + a\,\Delta + b\,\Delta^2}{1 + b\,\sigma_W^2}. \quad (9)$$

At the same level of accuracy Eq. (8) can be written as

$$G(W,W') = \frac{1}{\sqrt{2\pi}\sigma_W}\,\frac{1 + c\,(W-W')^2}{1 + c\,\sigma_W^2} \times \exp\left(-\frac{(W + \Delta W - W')^2}{2\sigma_W^2}\right), \quad (10)$$

with some parameter c and the energy shift

$$\Delta W = -a\sigma_W^2. \quad (11)$$

For a given energy scan this shift was constant, thus we did not take it into account in the scan analysis, but corrected the resulting mass value.

To determine the resonance mass we fitted the cross section measured in the energy scan using expressions (7) and (10) with four free parameters: the resonance mass M, the energy spread σ_W, the detection efficiency ε and the continuum cross section in the reference point $\sigma_{\text{cont}}^{\text{obs}}$. The c parameter was fixed at zero for the mass determination and released to find the systematic mass uncertainty due to the symmetric distortion of the energy distribution. All other parameters required for the computation were taken from the PDG tables [16].

5. Mean collision energy for e^+e^- beams

At the given collider energy E the mean invariant mass averaged over the colliding particle momenta can be written as follows:

$$\langle W\rangle_p \approx \langle E_+ + E_-\rangle - \frac{1}{2}(\theta_x^2 + \theta_y^2)E - \frac{\sigma_E^2}{2E} - \frac{(\langle E_+\rangle - \langle E_-\rangle)^2}{4E}, \quad (12)$$

where θ_x, θ_y determine the radial and vertical angular spread, respectively, and σ_E is the energy spread inside the beams. The last term is due to the difference of the coherent energy loss in two arcs. For the VEPP-4M conditions in the ψ-energy region the correction is about 0.2 keV, thus we assume $W = E_+ + E_-$ for each collision.

In this assumption for beams with the Gaussian spreads in the presence of the electrostatically induced vertical dispersion η_y and the beam impact parameter Δ_y, the differential luminosity can be written as

$$\frac{dL(E,W)}{dW} = \frac{f_R N_+ N_-}{4\pi\sigma_x(W/2)\,\sigma_y(W/2)}\cdot\frac{1}{\sqrt{2\pi}\,\sigma_W} \times \exp\left\{-\frac{1}{2}\left(\frac{W-2E}{\sigma_W} - \frac{\sigma_W\eta_y\Delta_y}{2E\sigma_y^2}\right)^2 - \frac{\Delta_y^2}{4\sigma_y^2}\right\}, \quad (13)$$

where f_R is a revolution frequency, N_+ and N_- are the bunch populations. The transverse beam sizes in the interaction point σ_x, σ_y effectively depend on the sum $E_+ + E_-$ due to the collider β- and dispersion function chromaticity. For the a parameter of Eq. (9) one has

$$a \approx \frac{1}{2}\frac{\beta_y'}{\beta_y} + \frac{1}{2}\frac{\beta_x'}{\beta_x}\frac{\sigma_{x,\beta}^2}{\sigma_{x,\beta}^2 + \sigma_{x,s}^2} + \frac{\eta'}{\eta}\frac{\sigma_{x,s}^2}{\sigma_{x,\beta}^2 + \sigma_{x,s}^2}. \quad (14)$$

Here η is the dispersion function in the interaction point which is nonzero at VEPP-4M. Because of this there are two contributions to the radial beam size, the betatron contribution $\sigma_{x,\beta}$ and the synchrotron one, which is related to the beam energy spread $\sigma_{x,s} = \eta\,\sigma_E$. There exists an accelerator technique to measure the first derivatives of the β-functions β_x' and β_y', at VEPP-4M its relative accuracy is about 25%. The derivative of the dispersion function can be obtained from the accelerator simulation, the expected accuracy is 50%. There are no methods for a determination of the second derivatives, therefore the value of the b parameter of Eq. (9) and the c parameter of Eq. (10) cannot be predicted. The impact of the β-function chromaticity on the mass values in our experiments varies from -4 to -1.5 keV for J/ψ and from 3 to 5 keV for $\psi(2S)$. The effect of the dispersion function chromaticity of about -2 keV was not accounted for in Ref. [8].

Eq. (13) shows that the collision energy averaged over particles of the beams differs from the sum of the beam energies by $\Delta W = \eta_y \Delta_y / (2E\sigma_y^2)\,\sigma_W$. According to the accelerator simulation of VEPP-4M, $|\eta_y| \approx 800$ μm. The electrostatically induced vertical dispersion is due to the beam separation in the additional (parasitic) interaction points (I.P.). The residual orbit perturbations related to this separation result in the beam misalignment in the experimental I.P. characterized by Δ_y. It can be controlled using the voltage on the electrostatic separation plates located near the interaction point. The small misalignment causes the relative reduction of the luminosity by $\Delta_y^2/(2\sigma_y^2)$, thus the uncertainty in the mean collision energy is determined by the accuracy of the luminosity tuning. The vertical beam size of VEPP-4M $\sigma_y \approx 7$μm, therefore for the tuning accuracy of about 2% the uncertainty on the collision energy does not exceed 10 keV. In the resonance mass uncertainty it is suppressed by a factor of $1/\sqrt{N}$ where $N > 100$ is the number of the tunings during the energy scan. In 2002 the tunings were performed manually after the collider filling. Since 2004 the a permanently running automatic procedure has been implemented.

6. Beam energy determination

The resonance depolarization method employs the relation between the spin precession frequency around the vertical guiding field of the storage ring Ω and the Larmor revolution frequency ω:

$$\Omega = \omega\left(1 + \gamma \cdot \mu'/\mu_0\right), \tag{15}$$

where γ is the Lorentz factor of the particle and μ'/μ_0 is the ratio of the anomalous and normal parts of its magnetic moment. For the electron this ratio is known with the relative accuracy of 2.3×10^{-10} [16]. The beam revolution frequency can be controlled and measured with the accuracy better than 10^{-8}.

The precession frequency can be determined by applying the external electromagnetic field of the slowly varying frequency Ω_D to the polarized beam in the storage ring. At the moment when Ω_D satisfies the condition

$$\Omega \pm \Omega_D = \omega \cdot n \tag{16}$$

with any integer n, the resonance depolarization occurs. Observing it with the polarimeter one determines Ω_D and thus Ω, γ and the beam energy.

In the energy region of J/ψ and $\psi(2S)$, the VEPP-3 booster serves as a source of the polarized beam for VEPP-4M. At this energy the spontaneous polarization time due to Sokolov–Ternov [17] effect in VEPP-4M is too large. The description of the VEPP-4M polarimeter which employed the intra-beam scattering (Touschek) effect can be found in Ref. [18]

The systematic uncertainty of the single energy calibration is limited mainly by the spin resonance width [6]. It can be determined using two calibrations with the opposite direction of the depolarizer frequency scan. In our experiments the resonance width does not exceed 2 keV. Another source of the uncertainty is vertical closed orbit distortions. Eq. (15) is exact in the case of the plane orbit in absence of the radial and longitudinal magnetic fields. The typical vertical orbit RMS at VEPP-4M was about 1 mm, the corresponding uncertainty in the energy determination was 1 keV or less [19]. The longitudinal field of the KEDR detector was compensated with high accuracy so that the uncertainty on the beam energy due to it is less than 1 keV [20].

The data acquisition scenario for all scans under discussion was similar to that described in Ref. [8]. According to it, the calibration of the beam energy was performed twice at each point on the peak region before and after the data taking. Only the energy of the electron beam was determined, thus the difference between the electron and positron energies $\Delta E_\pm$ was of great importance.

The energy obtained with the single beam resonant depolarization cannot be immediately applied to the data acquisition runs. During the data acquisition the beams must be electrostatically separated at all parasitic interaction points to increase the luminosity. In the case when the separation is turned on during the calibration (below we will refer to it as “calibration of type 1”), the correction to the additional vertical orbit distortion must be applied. This correction can be calculated accurately enough and is less than 1 keV, however, the electrostatic separation provokes the energy difference between the electron and positron beams. The controllable source of the difference is the skew sextupole NTS0 installed in the parasitic I.P. opposite to the experimental one. The total collision energy was corrected for its contribution (typically ± 1.5 keV) but there are also a few uncontrollable sources of $\Delta E_\pm$. Worrying about this, the “calibration of type 0” was suggested. In this case the separation is turned off during the resonant depolarization. Assuming that $\Delta E_\pm$ depends on the magnitude of the beam separation linearly and neglecting the difference in the orbit radius, one has

$$E_-^{\text{on}} = E^{\text{off}} - \Delta E_\pm/2, \qquad E_+^{\text{on}} = E^{\text{off}} + \Delta E_\pm/2,$$
$$E^{\text{off}} = (E_-^{\text{on}} + E_+^{\text{on}})/2,$$

thus the energy of the single beam with the separation off equals the mean energy of two beams with the separation on.

However, at the few keV level of accuracy, the difference in the orbit radius at the fixed revolution frequency f_R is not negligible. The correction required can be calculated with

$$\frac{\Delta E}{E} = \frac{1}{\alpha}\frac{\Delta R}{R} \approx -\frac{1}{\alpha}\frac{\Delta \mathcal{L}}{\mathcal{P}} \tag{17}$$

where ΔR is the change in the mean orbit radius, $\Delta\mathcal{L}$ is the orbit variation due to the separation at the condition that the radius does not change, $\mathcal{P} = c/f_R$ is the ring circumference and α is the momentum compaction factor of about 0.016. The maximal value of the correction is 7.4 ± 2.5 keV in the case of three parasitic interaction points. Some details of the calculations can be found in Ref. [21].

In two energy scans we used the “type 1” calibration, in the other “type 0” was employed. Recently the progress of the VEPP-4M polarimeter allowed us to verify the correction calculations experimentally with the accuracy of about 30% (2.5 keV at most). Similarly to the energy shift discussed in Section 4, the corrections which did not vary during the scan were applied to the resulting mass value.

Whatever type of calibrations were used, we had to interpolate their results to determine the energy during the data acquisition runs. This interpolation was done using the NMR measurement of the guiding field, the ring temperature and other accelerator parameters as described in Ref. [8]. During the early experiments the main magnets of VEPP-4M were cooled with the surrounding air, later water cooling was implemented. This decreased energy variations, but made them less predictable due to faster temperature variations. For both cooling methods the energy interpolation accuracy of about 6–8 keV was reached. The uncertainty of the energy extrapolation can be considered as quasi-statistical. Similarly to the uncertainty related to the beam misalignment, its contribution to the resonance mass uncertainty is suppressed proportionally to $1/\sqrt{N}$, but in this case $N > 100$ is the number of the collider fillings during the energy scan.

The value of energy obtained using the resonance depolarization corresponds to the average over the beam revolution time.

Table 1
Main characteristics of the data sets analyzed (the number of scans in the set, the integrated luminosity, the number of hadronic events selected, the machine energy spread, the separation state during the calibrations, the number of parasitic I.P.s, the skew sextupole state and the longitudinal magnetic field in KEDR).

Resonance	Year	N_{scan}	L (nb)	N_{hadr} (10^3)	σ_W (MeV)	Separation	N_{pIP}	NTS0	Field (T)
J/ψ	2002	4	50	16.5	0.90–0.66	off	1		0
	2005	1	205	109.0	0.68	on	3	on	0.65
	2008	1	486	615.0	0.71	off	3		0.60
$\psi(2S)$	2002	3	76	8.5	1.33	off	1		0
	2004	2	118	30.0	1.06	on	3	on	0.60
	2006	1	269	67.5	0.99	off, on	3	on	0.60
	2007	1	532	125.5	1.00	off	3		0.60

For a symmetric machine it corresponds to the energy in the interaction point despite the energy losses during the revolution. It is true, however, only when the potential energy of the beam particle can be neglected.

The effective energy of the electron is $E_{\text{kinetic}} + U/2$, where the potential energy U is due to its Coulomb interaction with all other electrons of the beam. For the flat beam with the logarithmic accuracy

$$U = \frac{e^2 N}{\sqrt{\pi}\,\sigma_z} \ln \frac{D}{\sigma_x}, \tag{18}$$

where N is the bunch population, σ_z is the longitudinal bunch size and D is the beam pipe diameter (in the beam rest frame the interaction of particles at longer distances is screened out). The kinetic and potential energies in the I.P. differ from those in the ring because of the difference in the beam and beam pipe sizes, but the total energy conserves during the revolution, therefore

$$E_{\text{kinetic,I.P.}} + U_{\text{I.P.}}/2 = E_{\text{kinetic,ring}} + U_{\text{ring}}/2. \tag{19}$$

Here energy losses during the revolution are ignored but it does not change the final results.

The resonant depolarization gives $E \approx E_{\text{kinetic,ring}}$, thus for the colliding e^+e^- pair we have

$$W_{\text{kinetic,I.P.}} = 2E + U_{\text{ring}} - U_{\text{I.P.}}, \tag{20}$$

$$W_{\text{total,I.P.}} = 2E + U_{\text{ring}} + U_{\text{I.P.}}. \tag{21}$$

In Ref. [8] it was assumed that at the moment of the annihilation the total energy of the e^+e^- pair transforms to the product mass, thus the correction $\delta W = U_{\text{I.P.}} + U_{\text{ring}} \approx 2$ keV was applied. However, some part of the potential energy $2U_{\text{I.P.}}$ can be radiated after the fast process of the resonance formation, therefore the value of the correction lies between $-(U_{\text{I.P.}} - U_{\text{ring}})$ and $U_{\text{I.P.}} + U_{\text{ring}}$. In this analysis we did not apply the correction for the beam potential increasing the systematic uncertainties on the resonance masses.

7. Data analysis

The data sets employed in the analysis and their characteristics essential for the mass determination are presented in Table 1.

The data collected in 2002 were not completely reanalyzed, just the mass values published in Ref. [8] were corrected and reweighted. The corrections were necessary to account for the dispersion function chromaticity effect mentioned in Section 5 (-2 and -3 keV for J/ψ and $\psi(2S)$, respectively), to withdraw the correction for the beam potential as discussed in the previous section (about -2 keV both for J/ψ and $\psi(2S)$) and, last but not least, to fix the technical mistake in accounting for the interference effect made in 2002. Namely, the square root was missing in the calculations of the interference parameters according to the first term of Eq. (6). Because of this the J/ψ mass was overestimated by 7 keV, while for $\psi(2S)$ the overestimation reached 16 keV (about 0.6 of the quoted error in both cases).

All other data were completely reprocessed. The luminosity was determined using Bhabha events with the scattering angle exceeding 15 degrees. The selection criteria for the hadronic and Bhabha events were similar to those described in Ref. [9]. During the $\psi(2S)$ scans performed in 2004 the liquid krypton calorimeter covering the angular range $37^\circ < \theta < 143^\circ$ was employed only in the trigger. The Bhabha events were selected using the CsI endcaps. The events containing at least three charged tracks were treated as the hadronic events provided that the sphericity parameter exceeded the value of 0.05. In all later scans the liquid krypton calorimeter was in full operation which allowed to increase the detection efficiency for hadronic events accepting events with two acollinear tracks and at least one photon.

The luminosity obtained using the process $e^+e^- \to e^+e^-$ was corrected for the resonance contribution using the table values of the electron width and the detection efficiency determined from Monte Carlo simulation. Such a correction is required to exclude the resonance mass shift due to the difference of the interference effects in the hadronic and e^+e^- channels. The maximal correction was about 15% for J/ψ and did not exceed 2% for $\psi(2S)$. The corresponding uncertainty on the J/ψ mass is about 1 keV.

The hadronic cross sections measured in the scans were fitted using the maximum likelihood method (the two $\psi(2S)$ scans performed in 2004 under the same detector and accelerator conditions were fitted together). The measured hadronic cross sections for J/ψ and $\psi(2S)$ scans and the results of the fits are presented in Fig. 2. The parameters of the fit are described in Section 4. The only fit parameter essential for this work is the resonance mass.

The mass values obtained for the data sets relative to the results published in 2003 (3096.917 and 3686.111 MeV for J/ψ and $\psi(2S)$, respectively) are presented in Table 2. The corrections to the mass due to the sum of accelerator-related effects considered in Section 4 and Section 6 are also shown to illustrate the difference of conditions significant for the mass measurements. They are already included in the quoted mass values.

8. Systematic uncertainties

The main systematic uncertainties on the J/ψ and $\psi(2S)$ masses and the estimates of their correlations are presented in Table 3 and Table 4, respectively. The correlation of errors is a difficult issue. In most cases we assumed that the correlated part corresponds to the minimal uncertainty in scans for a given uncertainty source. This leads to the most conservative estimates of the total uncertainty.

The energy spread variations are expected due to its possible dependence on the beam current. Evidence for such dependence was observed in 2002 but became much weaker later. The energy calibration accuracy and the energy interpolation for the data acquisition runs are discussed above in Section 6 together with the corrections due to the beam separation in parasitic interaction points. The energy difference of the electron and positron beams was studied using the simultaneous depolarization of e^+ and e^-

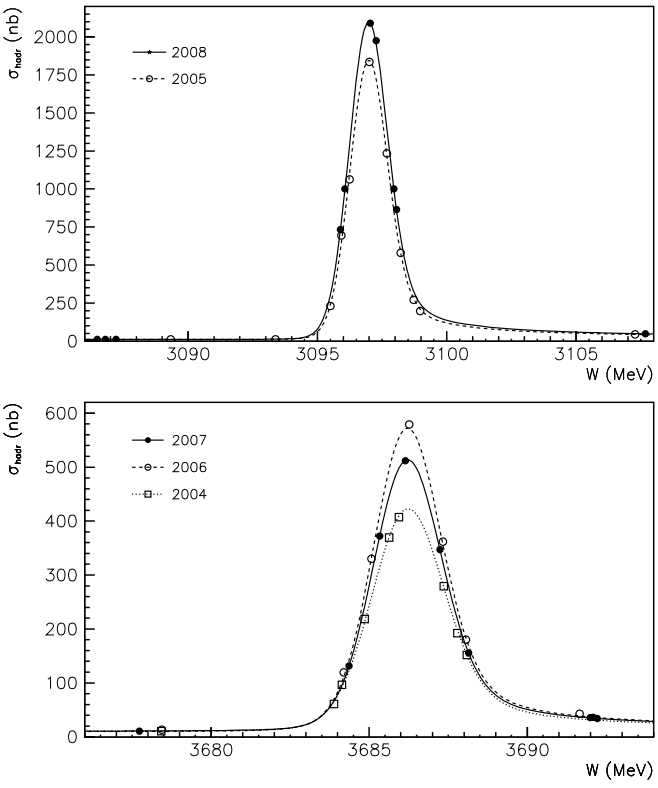

Fig. 2. The measured hadronic cross section not corrected for the detection efficiency as a function of the c.m. energy for J/ψ scans (top) and $\psi(2S)$ scans (bottom). The lines present the results of the fits.

Table 2
The mass values for the data sets relative to the results published in 2003 with their statistical uncertainties and the total corrections applied to the masses due to the accelerator-related effects.

Resonance	Year	$M-M_{2003}$ (keV)	ΔM (keV)
J/ψ	2002	-10.4 ± 10.0	-8.9 ± 1.9
	2005	-14.4 ± 3.1	-0.2 ± 2.1
	2008	-20.3 ± 2.7	-9.8 ± 2.3
$\psi(2S)$	2002	$-20.4 \pm 25.$	-2.0 ± 3.2
	2004	-0.5 ± 9.7	-0.5 ± 2.2
	2006	-11.0 ± 5.9	-3.0 ± 1.7
	2007	-15.9 ± 4.7	-7.1 ± 3.1

beams in the dedicated experiments. The asymmetric and symmetric distortions of the energy distribution correspond to the a and b parameters of the preexponential factor (9). The uncertainty due to the beam potential was evaluated as described in Section 6 using the mean values of the bunch currents. We estimated the contribution of the detection efficiency instability using a few alternative methods of event selection. A possible effect of the residual machine background was checked by relaxing the event selection criteria. The uncertainties appeared because the luminosity measurement instability was found comparing the mass values obtained using the luminosities from the two independent parts of the calorimeter. The correlated uncertainty mainly came from the correction for the resonance contribution to $e^+e^- \to e^+e^-$.

The essential uncertainties on the masses are related to the assumptions about the values of the interference parameter λ made in Section 3. To verify them we performed the joint fits of the two scans of J/ψ and the four scans of $\psi(2S)$ with floating λ. The fits resulted in

$$\lambda_{J/\psi} = 0.45 \pm 0.07 \pm 0.04, \qquad \lambda_{\psi(2S)} = 0.17 \pm 0.05 \pm 0.05$$

at the expected values of 0.39 and 0.13, respectively. The joint fits were not employed for the mass determination since the evaluation of systematic uncertainties became more difficult in this case. The alternative values of λ were used to obtain the mass values for each data set. The average values of the mass variations were considered as uncertainty estimates.

9. Weighting of results on masses

To perform averaging of the results on J/ψ and $\psi(2S)$ masses accounting for the partial correlation of systematic uncertainties we employed the procedure used in Ref. [9] for the leptonic width determination. The formal weighting prescription for the mass M is presented below:

$$\begin{aligned}
\langle M \rangle &= \sum w_i \cdot M_i, \\
\sigma^2_{\text{stat}} &= \sum w_i^2 \cdot \sigma^2_{\text{stat},i}, \\
\sigma^2_{\text{syst}} &= \sum w_i^2 \cdot (\sigma^2_{\text{syst,i}} - \sigma^2_{\text{syst},0}) + \sigma^2_{\text{syst},0}, \\
w_i &= 1/(\sigma^2_{\text{stat},i} + \sigma^2_{\text{syst},i} - \sigma^2_{\text{syst},0}),
\end{aligned} \tag{22}$$

where $\sigma_{\text{syst},0}$ denotes a common part of systematic uncertainties.

The weighting procedure gave the following results:

$$M^{J/\psi} - M^{J/\psi}_{2003} = -16.7 \pm 2.1 \pm 6.4 \text{ keV}, \quad P(\chi^2) = 0.59,$$
$$M^{\psi(2S)} - M^{\psi(2S)}_{2003} = -11.7 \pm 3.5 \pm 9.4 \text{ keV}, \quad P(\chi^2) = 0.68.$$

The χ^2 values are calculated taking into account the statistical uncertainties and the uncorrelated parts of the systematic ones.

Table 3
Systematic uncertainties on the J/ψ mass (keV).

Uncertainty source	2002	2005	2008	Common
Energy spread variation	3.0	1.8	1.8	1.8
Energy calibration accuracy	1.6	1.9	1.9	1.6
Energy assignment to DAQ runs	3.7	3.5	3.5	2.5
Beam separation in parasitic I.P.s[a]	0.9	1.7	1.7	0.9
Beam misalignment in the I.P.	1.8	1.5	1.5	1.5
e^+-, e^--energy difference	1.2	1.3[a]	1.2	1.2
Symmetric distortion of the energy distribution	1.5	1.3	2.1	1.3
Asymmetric distortion of the energy distribution[a]	2.1	1.9	1.9	1.9
Beam potential	1.9	1.9	1.9	1.9
Detection efficiency instability	2.3	1.7	1.8	< 0.1
Residual machine background	1.0	0.7	0.7	< 0.1
Luminosity measurements	2.2	1.7	1.7	1.1
Interference in the hadronic channel	2.7	2.7	2.7	2.7
Sum in quadrature	≈ 7.7	≈ 7.0	≈ 7.2	≈ 5.8

[a] Correction uncertainty.

Table 4
Systematic uncertainties in the $\psi(2S)$ mass (keV).

Uncertainty source	2002	2004	2006	2007	Common
Energy spread variation	2.0	1.5	1.5	1.5	1.5
Energy calibration accuracy	1.9	2.3	2.3	2.3	1.9
Energy assignment to DAQ runs	3.9	3.9	3.8	2.4	1.5
Beam separation in parasitic I.P.s[a]	0.5	1.2	1.7	1.7	0.5
Beam misalignment in the I.P.	5.1	3.3	3.3	3.3	2.5
e^+-, e^--energy difference	1.6	2.1[a]	2.1	1.6	1.6
Symmetric distortion of the energy distribution	1.8	1.6	1.6	1.6	1.6
Asymmetric distortion of the energy distribution[a]	2.1	1.9	1.9	1.9	1.9
Beam potential	2.0	2.2	2.2	2.2	2.0
Detection efficiency instability	2.1	1.6	1.6	1.6	< 0.1
Residual machine background	1.0	0.9	0.9	0.9	< 0.1
Luminosity measurements	3.0	2.1	2.1	1.5	0.7
Interference in the hadronic channel	4.1	4.1	4.1	4.1	4.1
Sum in quadrature	≈ 9.7	≈ 8.7	≈ 8.6	≈ 8.4	≈ 7.0

[a] Correction uncertainty.

The mass values obtained using different data sets are in good agreement. The exclusion of the data sets of 2002 which were not completely reanalyzed in this work shifts the mass values by -0.6 and $+0.3$ keV for J/ψ and $\psi(2S)$, respectively.

10. Summary

The analysis of KEDR data comprising six high precision scans of the J/ψ region and seven high precision scans of $\psi(2S)$ resulted in:

$$M_{J/\psi} = 3096.900 \pm 0.002 \pm 0.006 \text{ MeV},$$

$$M_{\psi(2S)} = 3686.099 \pm 0.004 \pm 0.009 \text{ MeV}.$$

These results should supersede our previous measurements published in 2003 (J/ψ and $\psi(2S)$) [8] and in 2012 ($\psi(2S)$) [9].

Acknowledgements

We greatly appreciate the efforts of the staff of VEPP-4M to provide good operation of the complex during long term experiments.

This work has been supported by Russian Science Foundation (project No. 14-50-00080). The investigation of the theoretical cross section in vicinity of a narrow resonance has been partly supported by the German Research Foundation (DFG) under grant HA 1457/9-1. The elaboration of the beam energy determination technique has been also supported in part by the RFBR (Grant No. 14-02-01011).

References

[1] M. Ablikim, et al., BESIII Collaboration, Phys. Rev. D 90 (2014) 012001.
[2] A. Tomaradze, et al., Phys. Rev. D 89 (2014) 031501.
[3] A. Tomaradze, et al., arXiv:1212.4191 [hep-ex].
[4] A.A. Zholents, et al., Phys. Lett. B 96 (1980) 214.
[5] A.D. Bukin, et al., Absolute calibration of beam energy in the storage ring, Φ-meson mass measurement, Preprint IYF-75-64, 1975.
[6] A.N. Skrinsky, Y.M. Shatunov, Sov. Phys. Usp. 32 (1989) 548.
[7] T.A. Armstrong, et al., E760 Collaboration, Phys. Rev. D 47 (1993) 772.
[8] V.M. Aulchenko, et al., KEDR Collaboration, Phys. Lett. B 573 (2003) 63.
[9] V.V. Anashin, et al., KEDR Collaboration, Phys. Lett. B 711 (2012) 280.
[10] K.A. Olive, et al., Particle Data Group, Chin. Phys. C 38 (2014) 090001.
[11] R. Aaij, et al., LHCb Collaboration, Eur. Phys. J. C 72 (2012) 1972.
[12] V. Anashin, et al., in: EPAC 98*, Stockholm, 1998, 1998, p. 400.
[13] V.V. Anashin, et al., Phys. Part. Nucl. 44 (2013) 657.
[14] E.A. Kuraev, V.S. Fadin, Sov. J. Nucl. Phys. 41 (1985) 466.
[15] S. Actis, et al., Eur. Phys. J. C 66 (2010) 585.
[16] J. Beringer, et al., Particle Data Group, Phys. Rev. D 86 (2012) 010001.
[17] A. Sokolov, I.M. Ternov, Sov. Phys. Dokl. 18 (1964) 1203.
[18] E.B. Levichev, et al., Phys. Usp. 57 (2014) 66.
[19] A.V. Bogomyagkov, et al., RUPAC-2006-MOAP02.
[20] S.A. Nikitin, RUPAC-2006-MOAP01.
[21] A.V. Bogomyagkov, et al., Conf. Proc. C 070625 (2007) 63.